Diffusion studies in nonequilibrium systems with attractive interactions

E. Arapaki,[1] P. Argyrakis,[1] and M. C. Tringides[2]
[1]*Department of Physics, University of Thessaloniki, 54006 Thessaloniki, Greece*
[2]*Department of Physics and Astronomy and Ames Laboratory, Iowa State University, Ames, Iowa 50011*
(Received 24 March 2000)

Diffraction experiments can be used easily to measure the time evolution of a system under nonequilibrium conditions to attain a new equilibrium state and deduce ''nonequilibrium'' surface diffusion coefficients. It is not clear how the ''nonequilibrium'' diffusion coefficients extracted from such diffraction experiments should be interpreted. We study with Monte Carlo simulations the behavior of the ''nonequilibrium'' tracer and collective diffusion coefficients in a lattice-gas model with attractive nearest-neighbor interactions, as the system evolves in time from an initial random state to attain the (1×1) ordered state for temperatures $T/T_c<1$. We calculate the dependence of the mean-square displacement $\langle R^2\rangle$ on time and the collective diffusion from the relaxation of the nonequilibrium structure factor $S(\vec{q},t)$ within time sub-intervals under the assumption that quasiequilibrium holds. We determine the time-dependent ''nonequilibrium'' diffusion coefficients and extract the time-dependent activation energies. For both diffusion coefficients the ''nonequilibrium'' values obtained at late times are compared to the corresponding values obtained at equilibrium.

I. INTRODUCTION

The study of the time evolution of a system under nonequilibrium conditions has been of great interest, both theoretically and experimentally, to identify the growth laws that apply. For example, systems initially in a disordered high-temperature phase evolve in time and form domains of the ordered phase, if they are quenched to a temperature $T/T_c<1$ below the critical temperature. Previous work has already answered several important questions relevant to the problem: how does the average size of the domains of the ordered phase grow in time, what is the domain size distribution as the domain size increases, etc. Most of these theoretically predicted results have been confirmed experimentally and are well documented in several reviews.[1–3]

Nonequilibrium experiments can be realized under different conditions, i.e., an arbitrary initial nonuniform concentration profile is set up, which smooths out with time as the atoms diffuse away. The final state of the system is one of uniform concentration. In the current study we restrict ''nonequilibrium'' to the conditions defined above: the system evolves in time from an initial random configuration to attain the ordered phase for $T<T_c$. Our goal is to relate results obtained in this type of nonequilibrium experiment to results obtained in equilibrium experiments. This does not mean that the diffusion coefficients extracted from the two types of experiments will be identical, since the configurations we are probing (random versus ordered) are different. However, we can determine how the measured activation energies can be explained in terms of the adsorbate-adsorbate interactions; conversely, once this relation is understood, we can answer one of the main practical questions in a diffusion experiment (i.e., how to deduce the potential energy surface and the adatom interactions), either from an equilibrium or a nonequilibrium experiment. Although our study is carried out in a specific model (i.e., the lattice-gas model with nearest-neighbor attractive interactions) and some of the results are specific to this model (as will be seen, there are some differences with a model which has competing, i.e., both attractive and repulsive interactions), the usefulness of the concept of a ''nonequilibrium'' diffusion coefficient and how to deduce the adatom interactions is a general one.

It has already been suggested that nonequilibrium experiments, carried out at different temperatures, can be used to extract information about the surface diffusion barriers.[4,5] This possibility is extremely appealing since such nonequilibrium experiments are easily carried out with diffraction [high-resolution low-energy electron diffraction (LEED)] in surface overlayers. Diffraction can monitor changes in the ordering of atoms on the surface. Correspondingly, theoretical studies of lattice-gas models have been the standard way to simulate the structure and dynamics of surface overlayers. The occupation variable $c_i=1$ (occupied) and 0 (empty) denotes whether the site i is occupied by an overlayer atom or not. The degree of order in the system is measured from the nonequilibrium structure factor defined by

$$S(\vec{q},t)=\frac{1}{(\theta N)^2}\left|\sum_i c_i(t)e^{i\vec{q}\cdot\vec{r}}\right|^2$$
$$=\frac{1}{(\theta N)^2}\left(\left|\sum_i c_i(t)\cos(\vec{q}\cdot\vec{r})\right|^2+\left|\sum_i c_i(t)\sin(\vec{q}\cdot\vec{r})\right|^2\right) \quad (1)$$

which is exactly what is measured in a LEED diffraction experiment, N is the number of sites on the lattice, and θ is the coverage.

It has been suggested that the temperature-dependent prefactor $A(T)$ appearing in the growth law for the average domain size

$$L=A(T)t^x \quad (2)$$

can be used to define a ''nonequilibrium'' diffusion coefficient $D \sim A(T)^{1/x}$, where x is the growth exponent for the time evolution. It is still not clear how this diffusion coefficient is related to the diffusion coefficient at equilibrium, i.e., when the ordered phase has been established in the system, with the domains reaching the size expected thermodynamically. However, diffusion experiments at equilibrium are notoriously difficult to perform and diffusion data at equilibrium are rather scarce.[6] Equilibrium measurements are based on the relaxation of small concentration fluctuations which are difficult to measure[7]; therefore, clarifying the relation between ''nonequilibrium'' and equilibrium diffusion coefficients is of high importance to legitimize the concept of a ''nonequilibrium'' diffusion coefficient, so diffraction experiments can be used as a substitute when results from equilibrium experiments are not available.

The standard definition of the collective diffusion coefficient at equilibrium is in terms of the relaxation of small-amplitude fluctuations of $S(\vec{q},t)$ in the long-wavelength limit $\vec{q} \to 0$, which are expected to decay to zero with time,

$$S(\vec{q},t) = S(\vec{q},0)\exp(-D_c t q^2), \tag{3}$$

or equivalently

$$D_c = -\frac{1}{q^2}\frac{d \ln S(\vec{q},t)}{dt} = -\frac{1}{q^2 S(\vec{q},t)}\frac{dS(\vec{q},t)}{dt}. \tag{4}$$

The definition can be extended in nonequilibrium systems if we divide the evolution time into sufficiently small subintervals, and assume that within each subinterval the system is at quasiequilibrium. This assumption is justified if the relaxation of the low-amplitude concentration fluctuations is faster than the domain growth time. The evolution process can be thought of as a series of successive relaxation experiments, with the state of the system in each experiment [i.e., with the initial value of $S(\vec{q},t)$, in each subinterval], defined by the nonequilibrium configuration of the system that has evolved according to the nonequilibrium growth laws and not thermodynamically. Thermal fluctuations generate deviations from the average domain morphology within each subinterval time. The system relaxes back to its average domain morphology via diffusion. Clearly thermodynamic information is lost in this type of experiment and, as will be discussed below, the measured ''nonequilibrium'' diffusion coefficient should be compared to the jump rate diffusion coefficient [since the experiment is not sensitive to the thermodynamic contribution to the collective diffusion coefficient, the thermodynamic factor $d(\mu/kT)/d \ln \theta$]. However, the experiment is still sensitive to the hops of the individual atoms (i.e., local hopping barriers), so it is still possible to relate the effective activation energies to the ones measured at equilibrium.

The relaxation of $S(\vec{q},t)$ within each time subinterval is governed by a relaxation expression as in Eq. (3). Since the average value of $S(\vec{q},t)$ and the domain morphology are different within each time subinterval and different atomic configurations are sampled in each time subinterval, this assumption will lead to a time-dependent ''nonequilibrium'' diffusion coefficient. Similar assumptions have been used to determine the ''nonequilibrium'' diffusion coefficient changes in a model with effectively competing nearest and next nearest neighbor interactions that describes the O/W(110) system.[5]

It is also of interest to measure the other key quantity in surface diffusion, namely the mean-square displacement

$$\langle R^2 \rangle = \frac{1}{N\theta}\sum_{i=1}^{\theta N} \delta R_i^2, \tag{5}$$

which defines the tracer diffusion coefficient. In systems at finite coverage with interactions between the atoms, the two diffusion coefficients measure totally different correlations and have a different dependence on the coverage and the temperature. We can define a ''nonequilibrium'' tracer diffusion coefficient during the evolution of the ordered phase domains to attain equilibrium in a similar way as in the definition of the ''nonequilibrium'' collective diffusion coefficient, by dividing the time evolution into subintervals and assume that within each subinterval quasiequilibrium holds. We can address the question of how the ''nonequilibrium'' tracer diffusion coefficient is related to the equilibrium one.

II. MODEL

We have studied an $L_0 \times L_0 = 61 \times 61$ lattice-gas model with attractive nearest-neighbor interactions J for $\theta = 0.5$, as the lattice gas is quenched from a high to a low temperature within the ordered phase $0.54 \leqslant T/T_c \leqslant 0.95$. The critical temperature is defined in terms of the interaction parameter $J/kT_c = 1.76$. The diffusion algorithm is based on the initial site energy (instead of the alternatively used Metropolis algorithm, which uses the difference in the energy between the initial and the final state): the probability of a randomly chosen atom to diffuse to a nearest-neighbor site (which is empty) is given by $p = \exp(-zJ/kT)$, where z is the number of nearest neighbors. As discussed earlier,[8] similar results for the domain size evolution are obtained for the two types of algorithms, but the single site energy algorithm is a more realistic representation of the diffusive dynamics in experimental systems (although it is slower than the Metropolis algorithm and results in smaller domain sizes, if the same number of MCS are used for the two algorithms).

This model has been extensively studied earlier to determine the time-dependent growth laws. Initial conflicting results about the value of the growth exponent x in Eq. (2) have been eventually settled in agreement with the expected value $x = \frac{1}{3}$ (from the Lifhsitz Slyozov theory[9]), if sufficiently long times are used in the simulations to attain the asymptotic time regime.[10] Growth is found to be self-similar (i.e., the evolving domain morphology obeys the same domain size distribution at all times), as evidenced from the scaling of the structure factor $S(q_m,t) = S_{\max} F(q_m/q_{\max})$, where $S_{\max}$ is the value of the structure factor at its maximum[9] max the corresponding wave vector and $F(x)$ is the characteristic scaling function.

In our simulations we have used times up to 10^5 MCS and since the emphasis is on the temperature dependence, we have covered a wide range of the quench temperature, deep within the ordered region. We have averaged 900 independent configurations, so even for the 61×61 lattice we have used, the accuracy is better than 1%. First we study the average mean-square displacement $\langle R^2 \rangle$ of all the particles ac-

cording to Eq. (5), which is well-defined independently of whether the system is at equilibrium or not. Although the standard definition of the tracer diffusion assumes that the long time limit is attained, it is still meaningful to study how the mean-square displacement $\langle R^2 \rangle$ changes with time, even for finite times, as the domains of the ordered phase evolve towards equilibrium.

We have divided the time over which the system evolves to attain equilibrium into subintervals (t_{n-1}, t_n) with $n = 1,2,3,4$ defined by the times t_n, and the constant values of $[\langle R(t_n)^2 \rangle = c_n]$ with $c_n = 15,30,60,100$. Both the choice of the intervals (defined by the constant values of $\langle R^2 \rangle$) and their specific values c_n's are rather arbitrary and are only used to determine how the activation energy of tracer diffusion changes with time. The tracer diffusion coefficient within each subinterval is defined by

$$D_n(T) = \frac{1}{4(t_n - t_{n-1})} [\langle R(t_n)^2 \rangle - \langle R(t_{n-1})^2 \rangle]. \qquad (6)$$

A practical advantage of this choice is that we use the same difference of displacements $[\langle R(t_n)^2 \rangle - \langle R(t_{n-1})^2 \rangle]$ for all temperatures. It is easier to implement this choice experimentally for methods that measure only $\langle R^2 \rangle$. A different definition of the selected times t_n' can be based on constant values of $S_{\max}$ (to be discussed next). This choice is equivalent to measurements of the tracer diffusion within time subintervals which have the same average domain size $L(t_n')$ (since, as will be discussed shortly, a constant value of $S_{\max}$ implies a constant value of L). For this choice of times we use different numerators in Eq. (6) for the different temperatures (i.e., mean-square displacement differences), but with this choice of times t_n''s, the system is at the same ''distance'' in phase space from the final equilibrium state. However, this construction is more difficult to implement in practice, since it requires experimental methods that measure $S_{\max}$ and $\langle R^2 \rangle$ simultaneously during the evolution of the system towards equilibrium. Since in the simulations we have this information (i.e., the time dependence of $\langle R^2 \rangle$ and $S_{\max}$ at the same time t), it is easy to relate the activation energies of the tracer diffusion extracted by the two different selection methods of the time subintervals.

The structure factor was calculated from Eq. (1) for all wave vectors $q_x = 2h\pi/L_0$ and $q_y = 2k\pi/L_0$, where h,k are integers varying independently from 0, $L_0 - 1$. Since $S(\vec{q},t)$ has azimuthal symmetry, it only depends on the magnitude of $\vec{q}$, so it was circularly averaged for all the pairs of values (h,k) satisfying the condition $m - 1/2 \leqslant \sqrt{h^2 + k^2} < m + 1/2$, with m ranging from zero to the nearest integer to $L_0/2$ and $q_m = 2m\pi/L_0$.

The shape and evolution of $S(q_m,t)$ with time contain all the information relevant to the evolving domain morphology. Its shape fully determines the domain size distribution and, as stated before, it has been shown to be self-similar. The area under the $S(q_m,t)$ is constant with time, $A = cS_{\max}q_{\max}^2$ [where c is a proportionality constant that depends only on the shape of $S(q_m,t)$, $S_{\max}$ is the maximum of the structure factor, and $q_{\max}$ is the wave vector corresponding to this maximum], as a result of the sum rule, i.e., the coverage is fixed at $\theta = 0.5$. This means no atoms are removed or added to the system. The average domain size L is the only necessary parameter to specify fully the domain morphology at any time t, because of the scaling of the structure factor. The time dependence of L can be obtained from different measures based on $S(q_m,t)$ (in addition to measurements of L from the mean chord intercepts in pictorials such as the ones shown in Fig. 1). For example, L is proportional to $1/q_{\max}$ or $S_{\max}^{0.5}$, or inversely proportional to the ith root of the ith moment of q_m, with $S(q_m,t)$ treated as a probability distribution.

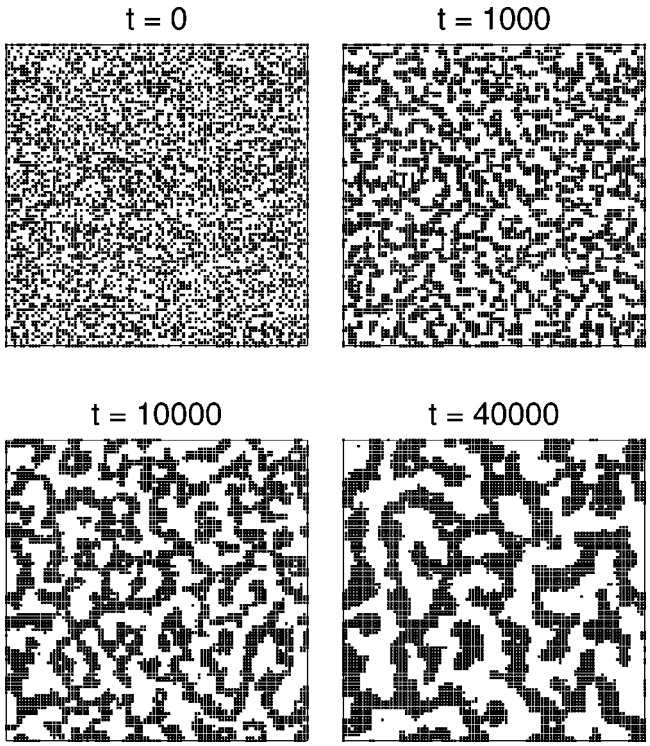

FIG. 1. Snapshots of the evolution of the domain configuration for different times after a quench of the system from $J/kT = 0$ to $J/kT = 3$. A lattice of size 101×101 with $\theta = 0.5$ is used. The average domain size for the latest configuration of 40 000 MCS, as measured from the linear domain chord, is 0.13 of the lattice size.

We have chosen to use the dependence of $S_{\max}$ versus t to monitor the increase of the average domain size since, usually, this is the easiest quantity to measure experimentally. We have determined $S_{\max}$ by using two different methods, because of the discreteness of the wave-vector grid q_m that we have used. At a given time, most likely the exact value $q_{\max}$ lies between the discrete values of q_m, so the correct value can be found by interpolation. With the first method the full structure factor $S(q_m,t)$ was calculated at a few finite times (~ 10 times) and the position of the maximum was determined by completing the bell-shaped top segment of the curve. Since $S(q_m,t)$ was calculated at discrete times, this provides only a finite set of the values of $S_{\max}$ versus t and it is difficult to calculate the slope $dS_{\max}/dt$ according to Eq. (4). Alternatively we have calculated the time dependence of $S(q_m,t)$ at fixed wave vector q_m for a larger number (closely spaced) of times, since it is easier computationally. At any given time the curve, corresponding to the value of q_m with the largest $S(q_m,t)$ value, was selected as an approximation to $S_{\max}$. With time the selected curve moves to the curve of

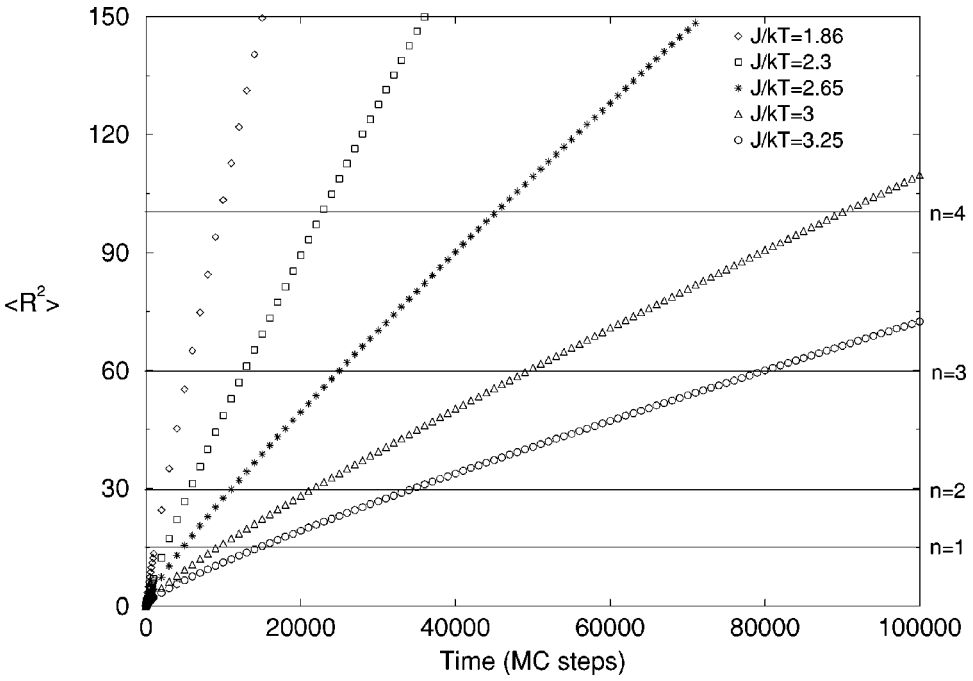

FIG. 2. Plot of $\langle R^2\rangle$ versus t for a lattice of size 61×61 with coverage $\theta=0.5$, for different values of temperatures in the range $0.54\leqslant J/kT\leqslant 0.95$. The horizontal lines $n=1,2,3,4$ correspond to the lines described in text for the calculation of the ''nonequilibrium'' tracer diffusion coefficient D_n, with times t_n selected for constant values of $\langle R^2\rangle$.

smaller wave vectors. This choice always underestimates the correct value of $S_{\max}$, especially at the cusplike features formed at the point of intersection of the $S(q_m,t)$ curves corresponding to two successive wave vectors. By comparing with the few discrete, more exact values that were interpolated from the full line shapes of $S(q_m,t)$, as discussed before, the maximum difference between the two methods is less than 10% (at the cusplike features) and becomes less pronounced with time. From these approximate $S_{\max}$ versus t plots, a power law was used for the fit to test $S_{\max}\sim A^2(T)t^{2x}$ (which effectively corrects for the approximation described above, since a power law is a monotonic function of time, with a smoothly varying derivative that smoothes out the cusplike features). The slopes $dS_{\max}/dt$ can be determined according to Eq. (4) with a much finer time grid for better accuracy.

Similar to the construction we have used to define the ''nonequilibrium'' tracer diffusion coefficient, we have selected the subintervals t_n' from the constant values of $S_{\max}=c_n'$ to define the collective diffusion coefficient, where $c_n'=0.002,0.004,0.008,0.012$ for $n=1,2,3,4$ (the corresponding values of the linear domain size as measured from the chord intercept show a change from 7% to 18% of the size of the system). Again this choice of c_n''s is rather arbitrary, but sufficient for the main interest of our study to show the time dependence of the ''nonequilibrium'' diffusion coefficient D_c and the corresponding changes of the activation energy with increasing n. As can be seen from Eq. (4), we can approximate D_c with simply the slope $D_c=(c/A)dS_{\max}/dt$, if we select as the wave vector of interest the wave vector of the maximum of the structure factor q_{max} [since the product in Eq. (4) $q_{\max}^2 S_{\max}=A/c$ for any n is constant, because of the sum rule satisfied by the integral of $S(q_m,t)$ noted earlier, i.e., the number of atoms on the lattice is fixed]. The slopes $dS_{\max}/dt$ at fixed n are proportional to the ''nonequilibrium'' collective diffusion coefficient $D_c=(c/A)dS_{\max}(T)/dt$ at the different temperatures T we have used. The constant c/A is independent of temperature and simply depends on the sum rule obeyed by $S(q_m,t)$. By plotting $dS_{\max}/dt$ versus $1/T$ for fixed n, we extract the activation energy of the ''nonequilibrium'' D_c as a function of n.

III. RESULTS

A typical picture of the domain evolution is shown in Fig. 1 for $J/kT=3$ and different times up to 40 000 MCS. We observe the typical fractal-like domain structure with the domains reaching sizes $L/L_0=0.13$ depending on the temperature. (The domain is measured from the linear chord length of straight line intercepts through the domains.)

$\langle R^2\rangle$ is shown in Fig. 2 for several temperatures $0.54\leqslant T/T_c\leqslant 0.95$. It is clear that the mean-square displacement does not follow a linear dependence on time, but its rate of growth decreases with time. This is a characteristic of anomalous diffusion with a sublinear time dependence of $\langle R^2\rangle\sim t^{1-x}$ with $x>0$. Earlier work[8] has shown that, for sufficiently low temperatures, the exponent x appearing in $\langle R^2\rangle$ is related to the growth exponent in Eq. (2) of L; so $\langle R^2\rangle$ can also be used to extract the growth laws of the nonequilibrium growth processes.

Figure 3 shows the Arrhenius plots for the ''nonequilibrium'' tracer diffusion coefficient as a function of n, the parameter that indicates how far the system has progressed towards the equilibrium state. These results are obtained with times t_n' defined by constant values of $S_{\max}$. The results obtained for times t_n defined by constant values of $\langle R^2\rangle$ are similar. It is important to emphasize that the data cover a very wide temperature range, far wider than most experimental studies that usually span a temperature range of a small percentage of T_c (typically less than 20%). The activation energy shows an increase (from $1.45J$ to $1.9J$) with n and is close to the expected value $2J=z\theta J$ (with $z=4$ the coordination number of the square lattice) for atoms with two nearest neighbors (which is the average coordination of the atoms at the domain boundaries). These are the only atoms that

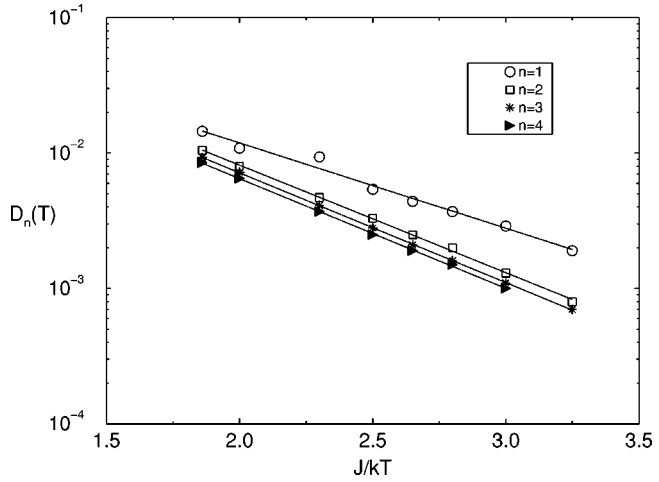

FIG. 3. Arrhenius plot of the ''nonequilibrium'' tracer diffusion coefficient $D_n(T)$ obtained with times selected from constant values of $S_{\max}$. The activation energies for the different time intervals corresponding to $n=1,2,3,4$ are $1.45J, 1.83J, 1.87J$, and $1.87J$.

contribute to the mean-square displacement in Eq. (5), since all the nearest-neighbor sites inside the domains are occupied and the inside atoms cannot diffuse.

Figure 4 shows the evolution of the circularly averaged structure factor $S(q_m,t)$ versus q_m for different times and $T/T_c=0.7$. It has the characteristic bell shape with the position of the maximum $q_{\max}$ shifting to smaller wave vectors, while the area under the curve remains constant with time.

Figure 5 shows the plot of $S_{\max}$ versus t covering one decade in the evolution of $S_{\max}$ and more than 2.5 decades in the time variation. The measured exponent shown in the figure increases slightly from 0.53 (for $T/T_c=0.95$) to as high as 0.6 as the temperature decreases (for $T/T_c=0.66$), approaching the asymptotic value $2x=2/3$ (at even lower temperatures the exponent seems to decrease again, because the probability for an atom to diffuse decreases according to the initial energy expression, so the kinetics are much slower and the domain sizes attained are smaller). The results show that we have not yet reached the truly asymptotic time regime that, as mentioned earlier, was notoriously difficult to

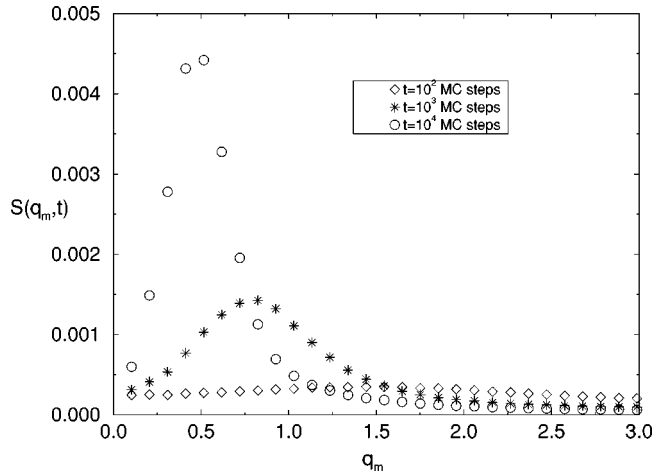

FIG. 4. Evolution of the circularly averaged structure factor $S(q_m,t)$ as a function of q_m, for three different values of time, $t=10^2, 10^3$, and 10^4 MC steps, $\theta=0.5$, $T/T_c=0.7$.

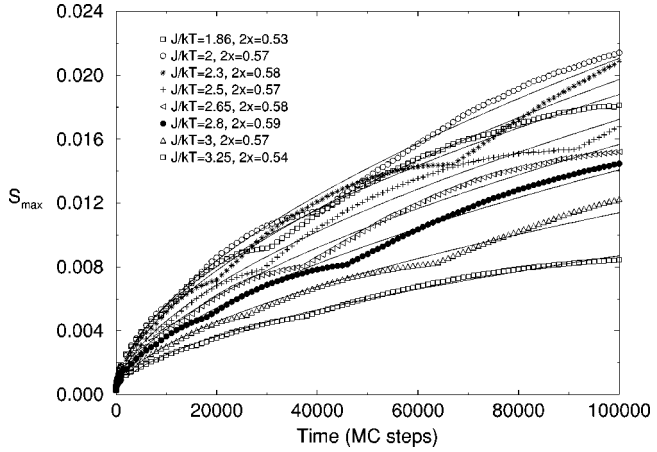

FIG. 5. Plot of $S_{\max}$ versus time for the temperature range $0.54 \leqslant T/T_c \leqslant 0.95$. The cusplike features are a result of the approximation used to determine $S_{\max}$ and are smoothed out with a power-law fit (which is expected to describe the evolution of $S_{\max}$). The extracted growth exponents are shown for the different temperatures and they approach the expected $\frac{2}{3}$ value.

attain. In earlier Monte Carlo studies[11] it was found that the growth exponent is $x=0.2$, smaller than the expected asymptotic value. Our study is beyond this regime, but still short from the asymptotic limit.

From the power-law expression Eq. (2) (and the relation between $S_{\max}$ and L) we extract also the prefactor $A^2(T)$. When $A^2(T)$ is plotted in an Arrhenius plot, we obtain the activation energy of $A^2(T)$, shown in Fig. 6, $2E_A=0.9J$. From this value and the conjectured expression relating the activation energy of $A^2(T)$ to the activation energy of the ''nonequilibrium'' diffusion coefficient $E_D=2E_A/2x$ (where $2x$ is the measured exponent from the growth of $S_{\max}$ versus t), we obtain the ''nonequilibrium'' diffusion activation energy $E_D=1.58J$ (using an average value of $2x=0.57$).

This value of the activation energy corresponds to the state of the system at the initial time of the evolution towards equilibrium $t=0$.[1] As discussed earlier, it is possible to de-

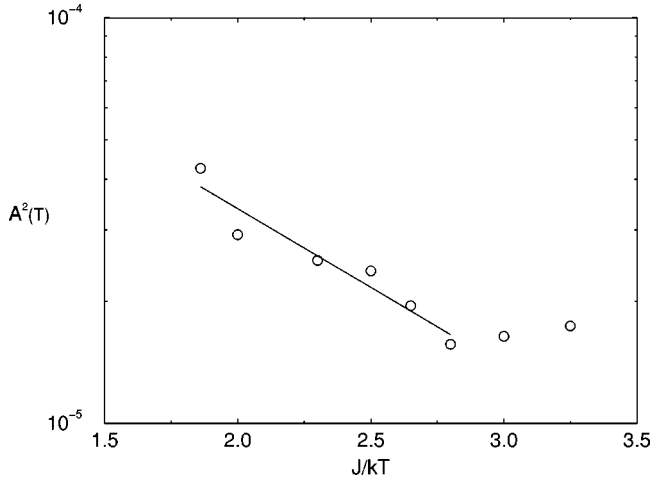

FIG. 6. Arrhenius plot of the prefactor $A^2(T)$ extracted from the power-law fits of Fig. 5. The extracted activation energy is $2E_A=0.9J$ which, using the conjectured relation relating the ''nonequilibrium'' diffusion activation energy to the growth rate activation energy $E_D=2E_A/2x$, results in $E_D=1.55J$.

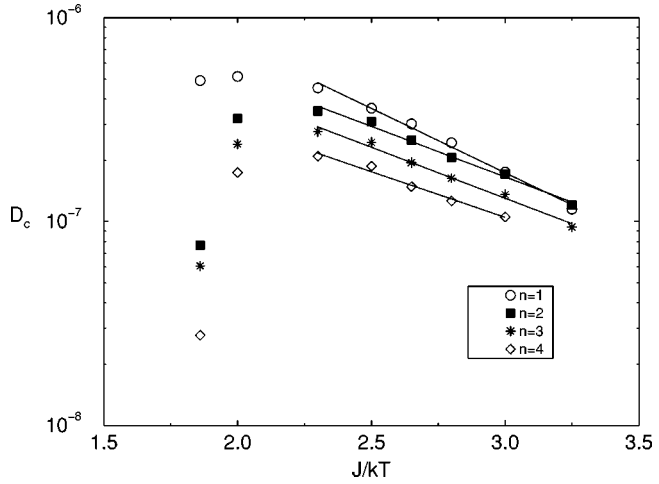

FIG. 7. ''Nonequilibrium'' collective diffusion coefficient D_c versus J/kT, for the time regimes extracted from the condition $S_{\max}=\text{const}$. The extracted activation energies are $1.45J$ for $n=1$, $1.14J$ for $n=2$, $1.15J$ for $n=3$, and $1.03J$ for $n=4$. The activation energy extracted for the early time interval $n=1$ agrees well with the one calculated in Fig. 6 from the growth rate $A^2(T)$, thus confirming the conjectured relation between the ''nonequilibrium'' and growth rate activation energies.

fine the ''nonequilibrium'' collective diffusion coefficient for different time intervals, as the system evolves in time from the initial random configuration towards the final ordered configuration of (1×1) domains, with a similar construction to the one used to extract the ''nonequilibrium'' tracer diffusion. The constant values of $S_{\max}$ we have chosen are rather arbitrary, since we are primarily interested to see the time dependence of $D_c(n)$. The ''nonequilibrium'' collective coefficient $D_c(n)$ is proportional to the slope of the $dS_{\max}/dt(n)$ defined at the same time t_n' based on Eq. (4).

Figure 7 shows the corresponding Arrhenius plots of the ''nonequilibrium'' collective diffusion coefficient for different temperatures and fixed n. Although the data do not obey an Arrhenius form over the entire temperature range we have used, it is clear that if we concentrate at the temperatures within the ordered region $(0.77\geqslant T/T_c\geqslant0.54)$, an Arrhenius form is a good fit. This is not surprising since, for temperatures close to T_c (and for longer time intervals $n>2$), fluctuations become more important. As the phase transition is approaches the domain size is smaller than the domain size attained at lower temperatures. This decreases the collective diffusion rate extracted from $S_{\max}$ and causes the deviations from the Arrhenius form at temperatures close to T_c. The extracted activation energy decreases from $E=1.45J$ to $E=1.03J$ as n increases from $n=1$ to $n=4$.

IV. DISCUSSION

As noted earlier from Fig. 3, the activation energies for the tracer diffusion coefficient show a very weak increase with n, as the system approaches equilibrium, with the value $E=2J$ for the late time interval $n=4$. Monte Carlo studies at equilibrium were studied in Ref. 13, but mostly at higher temperatures than the ones used in our work. They found that the Arrhenius plots of the tracer diffusion coefficient show two branches, one for the higher temperatures in the disordered region and one for the lower temperatures within a temperature range below T_c. Their lowest temperature was $T/T_c=0.73$, while in our work $T/T_c=0.54$. For the low-temperature branch the activation energy is essentially coverage-independent and for the coverage of interest of our study, $\theta=0.5$, the two activation energies for the two temperature branches are similar, $E=1.7J$.

This value is lower than the one we deduce from our ''nonequilibrium'' tracer diffusion simulations $E=2J$. There are several reasons for this discrepancy. In addition to the difference in the temperature range with Ref. 13, we checked whether the extracted activation energy with n depends on the method by which the subintervals were defined, i.e., at constant values of $\langle R^2\rangle$ or at constant values of $S_{\max}$. The times t_n' defined by the constant values of $S_{\max}$ will define different values for $\langle R^2\rangle$ from the ones defined by the use of the times t_n. We have determined the corresponding values of $\langle R^2\rangle$ for the time intervals defined by the times t_n', and ''nonequilibrium'' tracer diffusion coefficients were defined from the corresponding ratios in Eq. (6) (i.e., with this choice the nominators take different values for the different temperatures). Physically, as indicated before, the use of the times t_n' corresponds to configurations of the system, which have the same average domain size L (and therefore the system is at same ''distance'' in configuration space from its final equilibrium configuration) for all temperatures. This choice of subintervals corresponds to the use of much larger mean-square displacements than before (i.e., for example, for $J/kT=1.86$ the $\langle R^2\rangle$ value for $n=4$ increases to 400 from its original value 100), since at a fixed value of $S_{\max}$ the corresponding value of $\langle R^2\rangle$ is higher the higher the temperature is. The extracted values of the nonequilibrium tracer activation energies with this method increase from $1.45J$ to $1.9J$, with n increasing from 1 to 4. What is surprising is that in both cases (for constant $\langle R^2\rangle$ and $S_{\max}$ values), the final value of the activation energy is similar ($2J$ versus $1.9J$ correspondingly). The new value $1.9J$ is closer to the value $1.7J$ obtained by Ref. 13 in their studies of the tracer diffusion coefficient at equilibrium. Since at equilibrium the system has approached its final thermodynamically determined state and it has the same domain size (for all temperatures below T_c), the comparison with Ref. 13 is more meaningful for the choice of the time intervals with a constant value of $S_{\max}$ than $\langle R^2\rangle$.

The comparison of the ''nonequilibrium'' diffusion coefficient, extracted from $S_{\max}$ obtained in our simulations for the latest time interval $n=4$, $E=1.03J$, is better justified if we compare with their results for the jump rate diffusion coefficient. Their collective diffusion coefficient was obtained, from the well-known relation, as the product of the jump diffusion coefficient and the thermodynamic factor $[d(\mu/kT)/d\ln\theta]$.[12] The latter is purely an equilibrium quantity defined from the isotherm of the system, while the first quantity is defined in terms of the ratio of successful/attempted jumps averaged over all the atoms in the system. For the thermodynamic factor there is no equivalent quantity in a ''nonequilibrium'' experiment, since the thermodynamic variables do not obey the relation specified by the minimization of the free energy of the system, but are imposed by the initial disordered state the system is in. We do not expect our

''nonequilibrium'' collective diffusion to include any contribution from the thermodynamic factor, since the fluctuations present in a ''nonequilibrium'' experiment are generated by the evolving state of the system. The activation energy of the jump rate diffusion coefficient in Ref. 13 is weakly dependent on coverage and at $\theta=0.5$ it has a value of $E=1.7J$, but for temperatures much higher than the ones we have used in our study. Reference 13 covers the range $0.9\leqslant T/T_c\leqslant 7.0$ while we cover the range $0.54\leqslant T/T_c\leqslant 0.77$, so a direct comparison with the same temperature range is not possible. In their Arrhenius plot they have not included their lowest temperature point ($T/T_c=0.73$), because it has a value higher than the value expected from the $E=1.7J$ value of the activation energy. Based on the value of this point it is possible to deduce that, for temperatures within the ordered region, the activation energy decreases, and since our temperature range is well within the ordered region, it is consistent with the lower activation energy $E=1.03J$ we have measured from the dependence of $dS_{\max}/dt$ for $n=4$. It would be useful to have equilibrium diffusion data at lower temperatures to test if the lower value in our ''nonequilibrium'' simulations can be accounted for, since our ''nonequilibrium'' diffraction based method can only be used in the ordered region.

Even without the benefit of a full comparison with the equilibrium results, we can address the question of why for the ''nonequilibrium'' tracer diffusion coefficient the activation energy is almost constant with time and higher than the ''nonequilibrium'' activation energy of the collective diffusion coefficient which decreases with time. A qualitative argument can rationalize the result. For the ''nonequilibrium'' tracer diffusion coefficient, as discussed earlier, the temperature dependence of $\langle R^2\rangle$ is entirely determined by the detachment of atoms from the boundaries of the (1×1) ordered domains. These atoms diffuse in the empty region between the ordered domains, until they are captured by other domains present on the surface. This excitation requires the break up, on the average, of two nearest-neighbor bonds. For the ''nonequilibrium'' collective diffusion coefficient, it is also necessary to excite the same atoms at the domain boundaries to the empty region (but since the collective diffusion is measured from $dS_{\max}/dt$, the change of the domain size depends on the net flow of the atoms in the growing domains, i.e., the difference in the number of atoms which attach to, minus the number of atoms which detach from, the growing domains). This difference becomes less pronounced with time since, as the domains grow larger, the net fraction of atoms contributing to $dS_{\max}/dt$ decreases. Since the fraction of atoms added to the net growth of the domains (out of all the atoms excited from the domain boundaries) decreases with time, this reduces the temperature dependence of the number of atoms contributing to $dS_{\max}/dt$ and lowers the effective barrier measured in Fig. 7.

We can use our results to test the relation proposed for the ''nonequilibrium'' collective diffusion defined in terms of the prefactor $A(T)$ in Eq. (2) and the ''nonequilibrium'' collective diffusion coefficient defined in Eq. (4). As discussed earlier, we obtain a value $E_D=1.58J$ from the activation energy of the growth rate $A(T)$ ($E_D=2E_A/2x$ with deviations from Arrhenius plots at lower temperatures for the time intervals $n>2$), while the activation energy we obtain from the first time interval $n=1$ from Eq. (4) is $E=1.45J$. This verifies the proposed relation defining the ''nonequilibrium'' diffusion coefficient in terms of the growth ratio.

Our analysis of the activation energies on the lattice-gas model with attractive interactions has so far shown that the ''nonequilibrium'' results we obtain for the tracer increase weakly, while the collective diffusion decreases with the evolution of time, and they confirm the conjectured relation between the activation energy obtained from the collective diffusion coefficient and the activation energy obtained from $A(T)$.

''Nonequilibrium'' diffusion coefficients and activation energies were obtained in an earlier study,[5] on a lattice-gas model with competing interactions [which result at low temperature in the formation of a $p(2\times1)$ phase]; the phase consists of a series of fully occupied rows every two lattice spacings (or columns) separated by empty rows (or columns) in between. The lattice-gas model describes the well studied experimentally O/W(110) (Ref. 4) and reproduces most of the known results about the ordered phases present for different temperatures and coverages. The system was quenched from a high-temperature disordered phase to temperatures within the ordered region and the growth of the domains of the $p(2\times1)$ phase (which is fourfold degenerate) was monitored with time.[5] ''Nonequilibrium'' tracer and collective diffusion coefficients were determined from the times that the extra energy of the system (i.e., which is contained in the domain walls) decreases by a constant fraction. Since the extra energy in the system is inversely proportional to the average domain size, this choice is equivalent to the choice of time intervals with the same domain size or equivalently with constant values of $S_{\max}$. In this study the activation energies for both the ''nonequilibrium'' tracer and collective diffusion coefficients follow similar trends with time. They increase by approximately 0.3 eV from the initial $n=1$ to the final time subinterval $n=4$ used. The increase of the activation energy with time is consistent with the experimental results for the O/W(110), which show that the ''nonequilibrium'' activation energy obtained with LEED diffraction experiments is lower by 0.4 eV from the activation energy obtained in equilibrium fluctuation experiments. In addition, the activation energy measured in the simulations from the growth rate $A(T)$ versus $1/T$ Arrhenius plots is in good agreement with the value extracted from the relaxation of the $S(\vec{q},t)$ for the early time intervals ($n=2,3$) that show the growth exponent to have the expected value $x=\frac{1}{2}$. This again confirms the conjectured relation $E_D=E_A/x$ relating the ''nonequilibrium'' to the growth rate diffusion activation energies.

Comparison of our results to the ones of Ref. 5 show that the type of structure formed (i.e., how many vacant sites are present in the unit cell of the structure) is essential to understand the behavior of the activation energy with n. For close structures like (1×1) (which has zero vacancy factor for atoms inside the domains), the activation energy of the tracer diffusion does not change much, as we found in our study, simply because diffusion is controlled by the atoms at the perimeter of the domains. These atoms have approximately two nearest neighbors irrespectively of the size of the domains. This can explain why the activation energy we have found does not change substantially during the evolution of

the domains and why it has a value close to $2J$. For the ''nonequilibrium'' collective diffusion coefficient we have suggested earlier that the decrease of the activation energy with n might be related to the long-range diffusion, necessary for the atoms to reach the domains, and generate a positive flux to the growing domains.

On the other hand, for semiopen structures like $p(2\times1)$, the activation energy increases with n, since in this case hops are possible either from atoms inside the domains [i.e., atoms executing random walks in the $1-d$ corridors of the $p(2\times1)$ ordered phase] or from atoms at the domain perimeter. Since with time the fraction of atoms at the perimeter decreases, hops at late times are predominantly generated from the inside atoms. These atoms are formed from atoms breaking the attractive bonds at the walls of the ordered chains of the $p(2\times1)$ structure, which increases the activation energy.

The importance of the changing of local configurations with time and the role of atom hops from within the $1-d$ corridors of the $p(2\times1)$ ordered structure at late times were demonstrated in an earlier Monte Carlo study on a lattice-gas model that has a similar phase diagram to the O/W(110) system [although repulsive (instead of competing) interactions were used both for nearest- and next-nearest neighbor interactions].[14] It was found that the major contribution to the average hopping rate (i.e., averaged over all the local configurations that an atom experiences) was determined by atoms performing random walks within the $1-d$ corridors. These atoms have six repulsive bonds (i.e., four bonds for next nearest neighbors and two bonds for nearest neighbors). Despite the steady decrease of the fraction of atoms with this particular configuration with time (and temperature), these atoms have the largest contribution to the average jump rate. Additionally, an effective growth rate $A(T)$ was defined from the temperature dependence of the average domain size, but contrary to the definition of Eq. (2), the definition in Ref. 14 emphasizes the late time growth of the system. It is easy to see that this effective growth rate has higher activation energy than the activation energy obtained at early time (a result similar to the one found in Ref. 5). At late times the excitations of the atoms out of the walls of the $p(2\times1)$ structure are the main path for atoms to diffuse and contribute to the domain growth, while at early times their contribution is less important, since other atom configurations, which have a weaker temperature dependence, can contribute to the diffusion current.

V. SUMMARY

We have studied the two types of surface diffusion coefficients, the tracer and the collective diffusion under ''nonequilibrium'' conditions, while the system evolves in time to form domains of the (1×1) ordered structure. These two diffusion coefficients extend the usual definition of the corresponding coefficients at equilibrium by assuming that the system is at ''quasiequilibrium'' within sufficiently short time intervals during the evolution, i.e., local concentration fluctuations decay with the usual diffusion mode over a time scale shorter than the typical growth time of the domains. For the model we have studied in this work [which is based on nearest-neighbor attractive interactions and supports the formation of close (1×1) structures], we find that the ''nonequilibrium'' tracer diffusion activation energy depends weakly on time and agrees with the tracer activation energy results obtained at equilibrium. This results from the ''closeness'' of the ordered structure, so only atoms at the domain boundaries contribute to diffusion (since the atoms inside the domains cannot diffuse). The activation energy for the ''nonequilibrium'' collective diffusion coefficient cannot be compared to the one obtained at equilibrium, since the temperature range used in the two simulations is different; based on the limited data, it seems that the activation energy in the ordered region is lower than the activation energy in the high-temperature disordered phase. This decrease and the corresponding decrease of the ''nonequilibrium'' collective activation energy with time might be a result of the long-range diffusion necessary for the domains to grow. For the ''nonequilibrium'' diffusion coefficients obtained for the open structures $[p(2\times1)]$ in a different model, the activation energy increases with time because diffusion at late times requires the breaking of the attractive bonds of the $1-d$ chains of the (2×1) structure. The main conclusion of our studies is that the concept of ''nonequilibrium'' diffusion coefficient is well defined and is of practical value, since nonequilibrium experiments (with the use of diffraction) are easier to implement experimentally than equilibrium experiments. In general, the nonequilibrium results will be time-dependent and will approach in the long time limit the equilibrium results. For the specific model we have used (i.e., the lattice-gas model with nearest-neighbor attractive interactions), this approach happens relatively quickly, since the atoms at the domain boundaries of the (1×1) phase (formed as a result of the interactions) are the only ones which can diffuse. Even if the measured activation energies are different, especially at early times, they can be explained for by how the adsorbate-adsorbate interactions contribute to the different configurations. In practice, this means that one of the main goals of the diffusion experiments (i.e., to deduce the potential energy surface and the adatom interactions) can be carried out with the same success either with equilibrium or ''nonequilibrium'' experiments.

ACKNOWLEDGMENTS

Ames Laboratory is operated for the U.S. Department of Energy by Iowa State University under Contract No. W-7405-Eng-82. This work was supported by the Director for Energy Research, Office of Basic Energy Sciences. We also thank University of Paderborn (Germany) for a computing grant used to carry out part of the present calculations.

[1] M. C. Tringides, in *The Chemical Physics of Solid Surfaces and Heterogeneous Catalysis: Phase Transitions and Adsorbate Restructuring at Metal Surfaces*, edited by D. A. King and D. P. Woodruff (Elsevier, Amsterdam, 1994), Vol. 7, Chap. 6.
[2] O. G. Mouritsen, in *Kinetics of Ordering and Growth at Surfaces*, edited by M. G. Lagally (Plenum, New York, 1990).
[3] K. Heinz, in *Kinetics of Interface Reactions*, edited by M. Grunze and H. F. Kreuzer (Spinger Verlag, 1987).
[4] M. G. Lagally and M. C. Tringides, in *Solvay Conference on Surface Science*, edited by F. W. de Wette (Springer, Berlin, 1988), p. 181.
[5] I. Vattulainen, J. Merikoski, T. Ala-Nissila, and S. C. Ying, Surf. Sci. **366**, L697 (1996).
[6] *Surface Diffusion: Atomistic and Collective Processes*, edited by M. C. Tringides (Plenum, New York, 1997).
[7] D. Foster, *Hydrodynamic Fluctuations, Broken Symmetry and Correlation Functions* (Addison Wesley, Reading, MA, 1990).
[8] M. C. Tringides, C. M. Soukoulis, and P. Levenberg, J. Phys.: Condens. Matter **5**, 4721 (1993).
[9] I. M. Lifshitz and V. V. Slyozov, J. Phys. Chem. Solids **19**, 35 (1961).
[10] J. G. Amar, F. E. Sullivan, and R. D. Mountain, Phys. Rev. B **37**, 196 (1988).
[11] G. S. Grest and P. S. Sahni, Phys. Rev. B **30**, 226 (1984).
[12] G. E. Murch, Philos. Mag. A **43**, 871 (1981).
[13] C. Uebing and R. Gomer, J. Chem. Phys. **95**, 7636 (1991).
[14] K. A. Fichthorn and W. H. Weinberg, Surf. Sci. **286**, 139 (1993).